Cadernos Lab. Xeolóxico de Laxe
Coruña. 2011. Vol. 36, pp. 177 - 206 ISSN: 0213-4497

Las pegmatitas de Barroso-Alvão, Norte de Portugal: anatomía, mineralogía y geoquímica mineral

Pegmatites from Barroso-Alvão, Northern Portugal: anatomy, mineralogy and mineral geochemistry

MARTINS, T.[1] and LIMA, A.[2]

(1) Geology Centre-Porto University; Rua do Campo Alegre, 687; 4169-007 Porto, Portugal (tmartinsgeo@gmail.com)
(2) Department of Geosciences, Environment and Spatial Planning, Rua do Campo Alegre, 687; 4169-007 Porto, Portugal (allima@fc.up.pt)

Recibido: 13/12/2010 Revisado: 5/02/2011 Aceptado: 20/02/2011

Abstract

The Barroso-Alvão pegmatite field is located in the Variscan belt, in the western part of the Iberian Peninsula, Northern Portugal and it is recognised for its numerous and varied aplite-pegmatite intrusions. This is a rare-element aplite-pegmatite field with enrichment in Li, Sn, Nb>Ta, Rb, and P. Several hundreds of pegmatite bodies were identified and described in this field area intruding a variety of rock types including different metasedimentary, and granitic rocks. In this study we present the geology and mineralogy, and mineral geochemistry of different types of aplite-pegmatites bodies found at Barroso-Alvão. Their description was based on field observation, mineralogy, emplacement of the bodies and geochemical data. There were identified five different groups: intragranite pegmatites with major quartz, feldspar, muscovite, biotite, and minor tourmaline, beryl and garnet; barren pegmatites with quartz, feldspar, muscovite, and minor biotite, apatite, and beryl, among other accessories; spodumene pegmatites with spodumene, Nb-Ta minerals, and Mn-Fe-Li phosphates, along with other accessory mineral phases; petalite pegma-

tites with petalite, cassiterite, Nb-Ta minerals, Mn-Fe-Li-Ca-Al-Ce-U phosphates; and lepidolite pegmatites with albite, lepidolite, cassiterite and Sr-Al phosphate minerals.

Keywords: pegmatite, lithium, Barroso-Alvão, Hercinian orogeny, Portugal

INTRODUCTION

The Barroso-Alvão pegmatite field has been studied for more than twenty years, and it is recognised for a great number of aplite-pegmatite intrusions. The pegmatite field, located in the Trás-os-Montes e Alto Douro region, Vila Real district of Northern Portugal, covers portions of four 1/50 000 scale geological maps: 6A-Montalegre, 6B-Chaves, 6C-Cabeceiras de Basto, and 6D-Vila Pouca de Aguiar.

Barroso-Alvão potential was first recognised during a regional mapping and granite petrology programme where several spodumene aplite-pegmatite dykes were described (NORONHA, 1987). Several studies focussed on the mineralogy, geochemistry, petrology and exploration aspects of these spodumene-amblygonite bearing intrusions (e.g. CHAROY and NORONHA, 1988; DÓRIA et al., 1989; NORONHA and CHAROY, 1991; CHAROY et al., 1992; PIRES, 1995; AMARANTE et al., 1999; FARINHA and LIMA 2000; LIMA, 2000; CHAROY et al., 2001).

Later it was identified a suite of aplite-pegmatite bodies in which petalite is a dominant phase (LIMA et al., 2003 a,b,c). Following this discovery a more expansive project was undertaken in order to understand the Barroso-Alvão pegmatite field in its entirety, including its origins, petrogenesis and the distribution of different intrusive phases (MARTINS, 2009). Particular interest was given to the following aspects: the pegmatite's relationship with the hosting rock, their internal structure and morphology; petrography and mineralogical description; mineral geochemistry and evolution of the pegmatite bodies.

In this paper we divide the pegmatites of the Barroso-Alvão area into different groups and describe their anatomy, relation with the country rock, mineralogy and mineral geochemistry. We use the mineral geochemistry to evaluate the pegmatite degree of fractionation and the evolution trend in this pegmatite field.

GEOLOGICAL SETTING

The Barroso-Alvão pegmatite field is located in the Variscan belt, in the western portion of the Iberian Peninsula (Figure 1). It belongs to the Galicia-Trás-os-Montes geotectonic zone (FARIAS et al., 1987), close to the thrust that represents the southern boundary with the Central Iberian geotectonic zone. The studied pegmatite field is positioned to the West of the Penacova-Régua-Verin fault, one of the major NNE-SSW Variscan faults that affect the Iberian Peninsula.

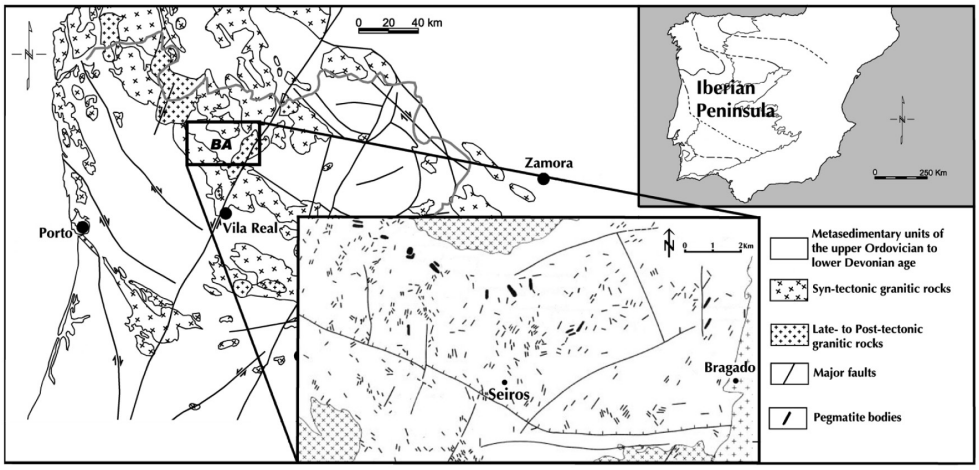

Fig. 1. Simplified geology map of the Barroso-Alvão region according to the 1/50 000 scale geological maps: 6A-Montalegre, 6B-Chaves, 6C-Cabeceiras de Basto, and 6D-Vila Pouca de Aguiar.

Metasediments and deformation

The main hosts of the pegmatites from Barroso-Alvão are meta-pelitic, mica-shists, and rarely carbonaceous or graphitic shists of upper Ordovician to lower Devonian age. RIBEIRO et al., 2000 subdivided the sequence into three distinct formations called unit Sa, unit Sb, and unit Sc based on metamorphic conditions and association of lithologies:

- Unit Sa is composed of phyllites and mica schists intercalated with carbonaceous or graphitic schists and some quartz phyllites and calcsilicate rocks.

- Unit Sb consists of quartzites and quartz phyllites interlayered with phyllites and some carbonaceous or graphitic schists. Lutites and graphitic schists occur in smaller proportions than in Unit Sa;

- Unit Sc is characterised by a relatively monotonous sequence of phyllites, mica schists and quartz wackes with rare calcsilicate rocks. Although rare, these calcareous rocks are important in differentiating the third unit from the previous units.

Three deformation phases (D_1 to D_3) were identified in the metasedimentary rocks in S_1 to S_3 superimposed schistosities. The S_1, S_2 and S_3 foliations observed in the field were produced during the three main ductile deformation phases of the Hercynian orogeny (D_1, D_2 and D_3) (NORONHA et al., 1981; DIAS and RIBEIRO, 1995).

First deformation phase (D_1) generated an axial planar foliation (S_1) that is well preserved at higher levels of the Galicia–Trás–os–Montes Zone. The S_1 foliation is parallel to the stratification ($S_1//S_0$) with main orientation N120º.

The D_2 is responsible for a sub-horizontal shear cleavage (S_2) that is locally upturned vertically by the D_3 phase.

The D_3 produced a locally strong, penetrative crenulation cleavage (S_3) that is preferentially associated with ductile shear zones (NORONHA et al., 1981). This was produced during the final Hercynian ductile upright folding event that resulted in the 120° trending folds, which overprint structures, related to phases D_1 and D_2.

Following D_3, brittle deformation generated important faults that affect the entire study area. The main trends of these fault systems vary from N020º - N030ºE to N-S, and E-W to ENE-WSW.

Metamorphism

The Central-Iberian Zone and the Galicia–Trás–os–Montes Zone have experienced intense and widespread granitic plutonism and metamorphism. MARTINEZ et al. (1990) delineated isograds of several metamorphic zones for the Iberian Massif. Their distribution is related to the regional metamorphism, closely related to granite plutonism that has been complicated by subsequent faulting events.

Within the study area it is possible to identify a synorogenic prograde metamorphism of medium to low pressure and high temperature. The metamorphism isograds are parallel to the contact of syntectonic granites and to the lithostratigraphic units. The isograds result from the Pre to Syn-D_3 regional thermal peak, related to prograde dynamothermal metamorphism (NORONHA, 1983; NORONHA and RIBEIRO, 1983; RIBEIRO et al., 2000).

Close to the contact with the syn-D_3 Cabeceiras de Basto granite there are two different mineralogical associations defining the andalusite isograde:

i) quartz + muscovite + biotite +/- andalusite +/- staurolite;

ii) quartz + muscovite + biotite +/- andalusite +/- staurolite +/- garnet +/- plagioclase.

A biotite isograd was also identified parallel to the andalusite isograde with three mineralogical associations:

i) quartz + muscovite + biotite;

ii) quartz + muscovite + biotite + chlorite;

iii) quartz + muscovite + biotite + albite +/- chlorite +/- garnet.

In addition to the regional metamorphism, we can distinguish a post-kynematic contact metamorphism related with post-D_3 granite magmatism and local, hydrothermal alteration related to aplite-pegmatite or quartz vein emplacement has also been recognised. It is inferred by a decussate texture in the phyllosilicates and the development of aluminosilicate porphyroblasts of andalusite and rarely sillimanite (fibrolite). Porphyroblasts of cordierite, garnet and biotite are also common. All porphyroblasts are Late- to Post-D_3, and some of them are restricted to the presence of quartz veinlets (RIBEIRO et al., 2007).

Granitic rocks

The region hosting the Barroso-Alvão pegmatite field contains several types of granitic rocks. In this work it is going to be used the classification proposed by FERREIRA et al. (1987), which takes into account he relationship of the granitic rocks and the Hercynian orogeny. In the field area, it is possible to identify Syn-D_3 granitoids and late to post tectonic granitoids (Post-D_3). Figure 2 shows a very simple and schematic division of the granites found in Barroso-Alvão.

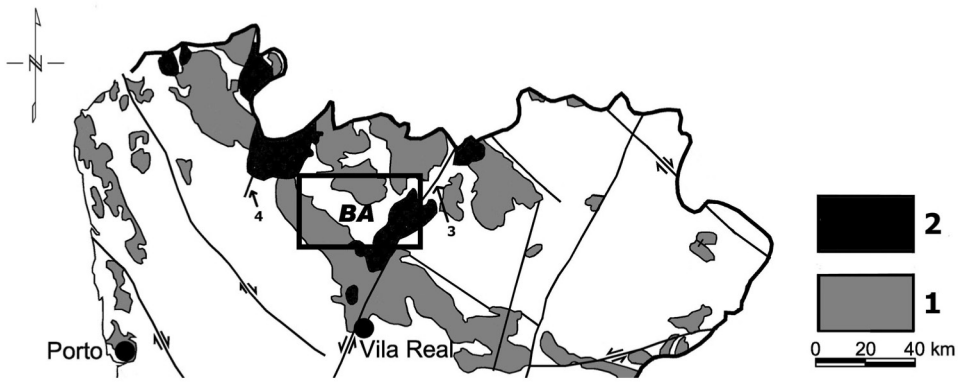

Fig. 2. Schematic representation of the different types of granitic rocks encountered at the Barroso-Alvão pegmatite field (BA). 1- Syn D3 granitoids; 2- Late to post tectonic granitoids (Post-D3); 3- Régua-Verin fault; 4- Gerês-Lovios fault. Adapted from FERREIRA et al. (1987).

The granitic rocks classified as Syn-D_3 define the boundaries of the study area to the north and southwest. In the north we find the Barroso granite (Syn to Late D_3) that is a two-mica granite, with a medium to coarse grained and porphyroid tendency. Petrographic study by NORONHA and RIBEIRO (1983) describes deformation especially apparent when the granite is close to the contact with the metasedimentary rocks. The major mineral phases are orthoclase (sometimes perthitic), albite-oligoclase, biotite (usually chloritised) and less abundant late muscovite. As accessories, apatite, tourmaline and opaque phases were described.

Towards the southwest we find the Cabeceiras de Basto granitic complex that is the most widespread in the study area and it is considered define the southwestern limit (Alvão) of the pegmatite field. According to FERREIRA et al. (1987), Cabeceiras de Basto is a two mica granitoid that is Syn-D_3 in age (Syn to Late D_3). The pluton complex intrudes lower Silurian metasediments along the core of a D_3 antiform defining a large NW-SE (N130º) trending structure. ALMEIDA (1994) described the mineral association for this granitic complex: quartz, anorthite, perthitic K-feldspar, biotite and muscovite; apatite, monazite, zircon, ilmenite, rutile, rare sillimanite and tourmaline occur as accessory minerals. The granites constituting the complex were subsequently deformed by late- to post-magmatic shear zones associated with significant hydrothermal alteration (ALMEIDA et al., 2002).

The geochemistry of the Cabeceiras de Basto granitic complex indicates almost identical peraluminous compositions ($1.2 < A/KCN < 1.4$). Fresh samples display short but well-defined chemical and mineralogical evolution trends that may be related to crystal fractionation of magmas during their emplacement. Li, Sn and W contents of the Cabeceiras de Basto granite allow their characterisation as 'specialised' granites (ALMEIDA, 1994).

The granitic rocks classified as Post-D_3 define the limits of the field area to the east. The Vila Pouca de Aguiar pluton is a composite massif elongated according to NNE-SSW direction. This pluton has not been

deformed and it is discordant relatively to the D_3 structures of the region: the two-mica syntectonic granite and the upper Ordovician to lower Devonian metasedimentary sequence (RIBEIRO, 1998). The elongated shape of this pluton extends in the same direction as the Penacova-Régua-Vein fault suggesting that its emplacement was controlled by this regional tectonic structure (MARTINS et al. 2009).

PEGMATITES FROM BARROSO-ALVÃO

Several hundreds of pegmatite bodies were identified and described in this field area (CHAROY et al. 1992, LIMA 2000, MARTINS 2009). They intrude a variety of rock types including several metasedimentary units, and different granitic rocks. In this study we present the different types of aplite-pegmatites bodies found at Barroso-Alvão (Table 1). Their description was based on field observation, mineralogy, emplacement of the bodies and geochemical data (MARTINS 2009). There were identified five different groups: intragranite pegmatites with major quartz, feldspar, muscovite, biotite, and minor tourmaline, beryl and garnet; barren pegmatites with quartz, feldspar, muscovite, and minor biotite, apatite, and beryl, tourmaline, chlorite, zircon, pyrite, and monazite-(Ce); spodumene pegmatites with spodumene, Nb-Ta minerals, apatite-(F), montebrasite, triphylite, phosphoferrite, dufrenite, fairfieldite, chlorite, tourmaline, zircon, uraminite and sphalerite; petalite pegmatites with petalite, cassiterite, Nb-Ta minerals, apatite-(F), montebrasite, ferrisicklerite, eosphorite, pyrite, sphalerite, uraninite, monazite-(Ce), autrenite, and xenotime; and lepidolite pegmatites with albite, lepidolite, cassiterite and Sr-Al phosphate minerals.

Table1: Different types of pegmatites that can be found at Barroso-Alvão pegmatite field.

Type	*Mineralogy*		*Relation with the hosting rock/ Metamorphism*	*Morphology and structure*	*Other features*
	Major	*Minor*			
Intra granite	Qtz Kfs Ms	Ab Bt Tur	Intrude the Cabeceiras de Basto granitic complex.	Internal zoning; Main orientations: N010ºE and N130ºE	Tourmaline layering in the contacts and crossing the pegmatite.
Barren	Qtz Kfs Ab Ms	Bt Chl Tur Ap	Intrude Sa, Sb and Sb unit; located in the andalusite and biotite isograde; tourmalinisation occurs in the metasedimentary rocks near the contacts with the pegmatite bodies.	No obvious zoning although quartz-rich zones are observed.	Located close to the granite but intruding metasedimentary rocks.
Spodumene	Ab Kfs Qtz Spd	Ap-(F) Mnt Pet CT	Intrude Sb unit; located in the andalusite isograde; tourmalinisation occurs in the metasedimentary rocks near the contacts.	No internal zoning; aplite and pegmatite unit are a textural feature; Discordant with D_3; usually concordant with D_2.	Major study done by previous authors based in outcrop and extensive drill core.
Petalite	Pet Ab Ms Qtz	Mnt Spd Cst CT	Intrude Sb and Sc unit; located in the andalusite and biotite isograde; tourmalinisation without preferential orientation in the contacting hosting rock; "pinched and swelled" quartz veins occur in the metasediments near the contact.	No obvious internal zoning although couplets of aplite and pegmatite are observed; usually discordant with D_3 structures although concordant with D_2.	The maximum length for observation of exposed outcrop was 2.80 m; Nigerite described on contacts drill core description and sampling.
Lepidolite	Lpd Ab Qtz	Ms Cst CT	Intrude Sb unit; located in the biotite isograde; tourmalinisation in the host rocks.	No complicated internal zoning observed. Discordant with D_3; usually concordant with D_2.	Intense weathering; sugary albite is the major component of the pegmatitic body.

Sa, Sb, and Sc are metasedimentary units defined by RIBEIRO et al. (2000). (For detailed description see Geological setting). Qtz- quartz, Kfs- K-felspar, Ms- muscovite, Ab- albite, Bt- biotite, Tur- tourmaline, Chl- chlorite, Ap- apatite, Spd- spodumene, Mnt- montebrasite, Pet- petalite, CT- columbite-tantalite, Cst- cassiterite, Lpd- lepidolite.

Intragranite pegmatites

The studied pegmatite bodies outcrop in the Cabeceiras de Basto granite and in the Barroso batholith (all Syn-D_3 granitic bodies). Intragranite pegmatites are barren and composed of quartz, K-feldspar, Na-rich plagioclase, muscovite and biotite as major mineral phases; tourmaline, apatite, chlorite, beryl, and garnet as accessory mineral phases; and trace amounts of zircon, and iron oxides. This type of pegmatite frequently shows internal zoning with concentration of quartz in the centre (an incipient quartz core), and K-feldspar and muscovite in the margins. The muscovite and K-feldspar usually develop comb structure, growing perpendicular to the walls of the pegmatite, as it is possible to see in Figure 3. Tourmaline, when present, can either define a layering in the margin of the pegmatitic body or in the host rock or can appear completely spread without any order or alignment.

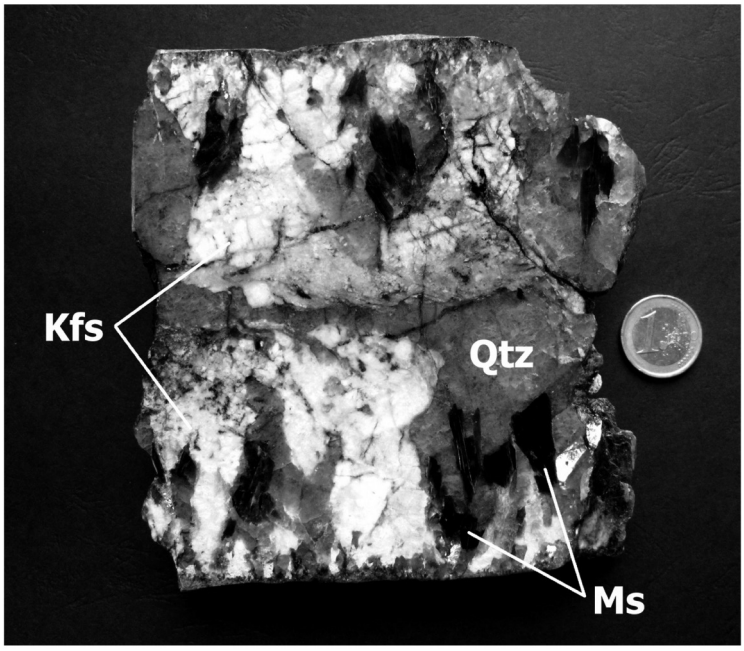

Fig. 3. Polished surface of an intragranite pegmatite. It is possible to observe muscovite (Ms), K-feldspar (Kfs) and quartz (Qtz) growing perpendicular to the walls of the pegmatite. Qtz is accumulated in the middle of the pegmatite. (The coin is used for scale.)

Barren pegmatites

Barren pegmatites are intruded into phyllites and mica schists metasedimentary units. They can be located close to the contact with the Cabeceiras de Basto massif but they are also found spread throughout the pegmatite field. The metamorphic conditions of the metasedimentary rocks correspond to the andalusite or biotite isograde. These types of pegmatites frequently show associated aplitic facies and rarely present a crude layering. The aplites are composed of quartz, K-feldspar, plagioclase and mus-

covite. The pegmatitic facies of the barren pegmatites is composed of quartz, K-feldspar, Na-rich plagioclase and muscovite. Accessory mineralogy consists of biotite, chlorite, tourmaline, apatite, garnet, zircon, pyrite, monazite, and Fe oxides.

Some pegmatites from this group frequently show incipient internal zoning with quartz concentration that resemble an incipient quartz core, and growing of K-feldspar and muscovite perpendicular to the walls. Different textural units with predominant quartz and muscovite are observed. Units with K-feldspar as the dominant mineral phase are frequently observed as well, although they are not present in all the studied pegmatites. K-feldspar goes up to 20 cm in length and it is fractured. Crude layering of garnet is often observed.

Spodumene pegmatites

Pegmatites with spodumene were the first lithium-bearing bodies described at the Barroso-Alvão pegmatite field (NORONHA, 1987). The initial discovery report was followed by several studies focused on spodumene aplite-pegmatite bodies (e.g. CHAROY and NORONHA, 1988; NORONHA and CHAROY, 1991; CHAROY et al., 1992; FARINHA and LIMA 2000; LIMA, 2000). According to CHAROY et al. (1992, 2001) this type of pegmatite bodies is unevenly distributed. They form local swarms of several bodies of various sizes up to 100 meters in outcrop width. Their average thickness is variable, from less than a few meters up to ten meters across. All pegmatites display irregular patterns in outcrop: some are flat lying; others have gently or steeply dipping attitudes along strike. The largest occurrence usually pinches and swells in accordance with the ductility of their hosting rocks and a large majority of these bodies exhibits a structural control.

The orientation of the pegmatites is mainly controlled by the S_2 foliation, which has been locally deformed by D_3 (striking at 120°E on average). The internal structure of the pegmatitic bodies is not easy to establish and they are considered internally unzoned. Textures were locally described as aplite-pegmatite couplets that alternate rhythmically. A contemporaneous aplitic unit is randomly and intimately mixed with a largely granular pegmatitic unit. The contacts between the pegmatite bodies and enclosing schists are sharp. Tourmalinisation was observed in the meta-pelitic units but there is no visible metasomatic alteration of the walls (CHAROY et al., 1992).

LIMA (2000) describes and characterises three of these spodumene pegmatite bodies. K-feldspar, quartz, spodumene and muscovite are the main mineral phases. Montebrasite, triphylite, fluorapatite, dufrenite, phosphoferrite, fairfieldite, interstitial petalite, tourmaline, eucryptite, illite, montmorillonite, chlorite, cookeite, sulphides, and organic matter are the accessory phases. Abundant petalite, beryl, columbite-tantalite, pyrite and uraninite were later described by MARTINS (2009).

Petalite pegmatites

Petalite pegmatites are intruded in a metasedimentary sequence composed of phyllites, mica schists and quartz wackes. The petalite pegmatites are composed of an aplitic and pegmatitic unit. Like the spodumene pegmatites, internal structure is difficult to establish, so they are considered internally unzoned with randomly and inti-

mately mixed texture of the aplite and the pegmatite units. Locally it was described a vertical zoning of aplite-pegmatite couplet texture that alters rhythmically. Petalite pegmatites are composed of petalite, Na-rich plagioclase, quartz, K-feldspar and muscovite as major mineral phases (Figure 4). As for accessories, montebrasite, spodumene, fluorapatite, cassiterite, columbite-tantalite, SQUI (isochemical breakdown of petalite to spodumene plus quartz described by ČERNÝ and FERGUSON, 1972), beryl, eucryptite, cookeite, ferrisicklerite, and Fe and Mn oxides are observed; trace amounts of zinnwaldite, montmorillonite, pyrite, zircon, monazite, uraninite, sphalerite, bastnaesite, eosphorite, thorite, and loellingite.

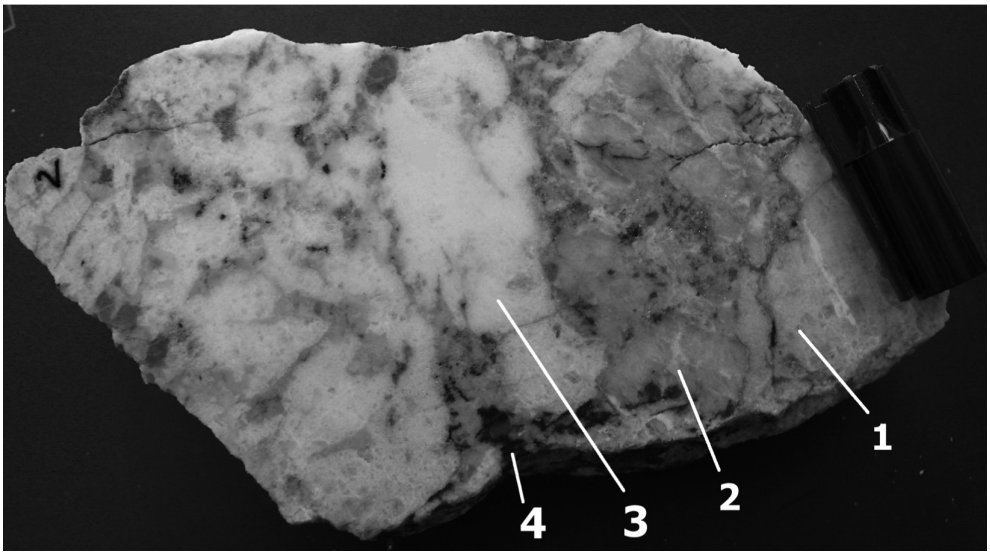

Fig. 4. Hand sample of a petalite pegmatite. 1- petalite crystals; 2- mass of feldspars; 3- white masse of cryptocrystalline petalite; 4- Mn oxide.
(The pen cap is used for scale)

Lepidolite pegmatites

In Barroso-Alvão, pegmatites with lepidolite are limited to two occurrences: CHN26 and CHN27, described by CHAROY et al. (1992). The brief reference to these pegmatites mainly focuses their strong enrichment in Li, Rb and F, based on whole rock geochemistry. MARTINS (2009) studied a body with lepidolite mined out for tin and with an outcrop reduced to barely a dump and it is exposed to severe weathering. Samples collected from this outcrop reveal the pegmatite is composed of fine- to medium-grained weathered (almost sugary) albite, fine- medium- to coarse-flaked pale violet to pink lepidolite, and quartz. Muscovite, cassiterite, apatite and beryl are accessories. Trace amounts of columbite-tantalite, zircon and goyazite are identified.

METHODOLOGY

Petrographic study was carried out on a Nikon Eclipse E 400 POL polarising microscope equipped with transmission and reflection light (objectives LU Plan 5x/0.15 POL ∞/0 EPI; 10x/0.30 POL ∞/0 EPI; 20x/0.45 POL ∞/0 EPI; and 50x/0.80 POL ∞/0 EPI). Software Axiovision 3.1. was used for photographic recording.

Representative samples of each type of pegmatite were crushed to centimetre size and then reduced to millimetre size. Crushing was followed by a heavy mineral separation using lithium metatungstate. The corresponding heavy (> 2.80 g/ml) and light fractions (< 2.80 g/ml) were examined under a binocular microscope, mounted in round disks, polished and analysed. Scanning Electron Microscope Energy dispersive spectral analysis, and BSE images of polished mounts and mineral samples affixed to conductive putty were collected using a digital AMRAY 1820 scanning electron microscope. Operating conditions for energy dispersive spectral analysis, and BSE imagery included an acceleration potential of 15-25 kV, 400 micron final aperture, 18 mm working distance, 0 to 35 degrees sample tilt, and 3.0 spot size. BSE images were collected using a frame size of 512x512 pixels and X-ray maps collected at 256x256 pixels with a 20-50 ms dwell time per pixel. Data and images were acquired using Iridium/EDS2008 software by IXRF Systems, Inc.

Electron microprobe analyses were carried out on a ARL SEMQ Electron Microprobe. Operating conditions for feldspars, micas, and phosphates included: 15 kV acceleration potential, 15 nA beam current and 60 seconds counting time. Mean Atomic Number (MAN) was used for background determinations as described (Donavan and Tingle, 1996). A 1-2 micron beam diameter was used for feldspars, micas and phosphates. For beam sensitive phosphates the beam diameter was adjusted to 3-4 microns. Standards used for analyses of feldspars, micas and phosphates included: Clinopyroxene (Si Kα, Fe Kα, Ti Kα, Ca Kα, Mg Kα), Albite (Si Kα , Al Kα, Na Kα), Fibbia adularia (Si Kα, Al Kα, K Kα), Plagioclase An50 (Si Kα, Al Kα, Ca Kα), Cerro de Mercado apatite (P Kα, Ca Kα, F Kα), Fayalite (Si Kα, Fe Kα), Rhodonite (Si Kα, Mn Kα), Andalusite (Si Kα, Al Kα), Fluortopaz (Al Kα, Si Kα, F Kα), Strontium sulfate (Sr Lα), Barium sulfate (Ba Lα), Pollucite (Cs Lα) and Rubidium Leucite (Rb Lα). Standards for feldspars, micas, and phosphates included: Periclase, hematite, vanadium (V) oxide, zinc oxide, quartz, fluorite, as well as any of the above where applicable.

Operating conditions for Nb-Ta oxides included: 25 kV acceleration potential, 20 nA beam current and 60 seconds counting time. MAN was used for background determinations. A 2-3 micron beam diameter was used for analyses of Nb-Ta oxides. Standards used for analyses of Nb-Ta oxides: Zirconium (IV) oxide (Zr Lα), manganotantalite (Ta Mα, Mn Kα), yttrium niobate (Nb Lα), Tin (IV) oxide (Sn Lα), Hematite (Fe Kα), rutile (Ti Kα), Bismuth germanate (Bi Mα) and Lead (II) oxide (Pb Mα). MAN standards for Nb-Ta oxides included: Periclase, hematite, vanadium oxide, quartz, fluorite, zinc oxide, Harding microlite, as well as any of the above where applicable. Data were processed via Probe for Windows by MicroBeam, Inc.

Lithium was measured in muscovite, K-feldspar and lepidolite separates using a Beckman Spectraspan V, Direct-Coupled

Plasma (DCP). The mineral separates were ground into powder. A sample of 200 mg was diluted in 0.035 l of hydrofluoric acid (HF). The wavelength used for Li was 610.362 nm and the counting time was 10 seconds; detection limit for Li= 0.002 mg/l.

RESULTS AND DISCUSSION

The mineralogy of the different groups of pegmatites is variable and becomes more complex from intragranite pegmatites to lepidolite pegmatites. Quartz, feldspars and muscovite are always present, but minerals such as tourmaline, garnet, and phosphates, spodumene, petalite and lepidolite, are only present in certain groups of pegmatites. The petrographic characteristics of the identified minerals are listed in Table 2. In this section we present the mineral geochemistry of various mineral phases of the studied pegmatites.

Feldspars

Feldspars are present in all the studied pegmatitic bodies. In intragranite, and barren pegmatites, K-feldspar is dominant over albite. On the other hand, in spodumene, and petalite pegmatites, albite is dominant over K-feldspar. In lepidolite pegmatites, K-feldspar is not present and albite is the only identified feldspar.

Petrographic characteristics for the feldspars from the different types of pegmatites can be found in Table 2. Representative analyses are available in Table 3 and 4. The analysed K-feldspar from the studied pegmatites has very similar composition and it is almost pure orthoclase (%Or= 93 – 99). As it is possible see in Table 4, the studied albite from the different types of pegmatites also has a similar chemical composition. It is very close to the albite end member. Anorthite percentage variation for the studied pegmatites is as follow: intragranite pegmatites- (An_{0-1}), spodumene pegmatites- (An_{0-3}) (CHAROY et al., 2001; LIMA 2000), petalite pegmatites- (An_{0-1}) lepidolite pegmatites- (An_0).

We anticipated that the trace element content of these feldspars would allow us to trace fractionation and evolution in the pegmatitic field. We predicted that the feldspars associated with the less evolved intragranite pegmatites were going to be the poorest in Rb and Cs, and show higher K/Rb ratios than those from the Li-rich (spodumene, petalite, and lepidolite pegmatites). The Li-enriched ones were predicted to have the feldspars richest in Rb and Cs, and one of the poorest in Ba and with the lowest K/Rb ratios, as showed in the literature by many authors (e.g. RODA-ROBLES 1993; NEIVA 1995; LARSEN 2002; ALFONSO 2003). P_2O_5 in feldspars was also measured once it can be considered a sign of evolution and can represent the amount of this element in the pegmatitc melt.

Table 2. Petrographic variety of the most important minerals found in the studied pegmatites.

Min	*Var*	*Petrographic characteristics*	*Pegmatite*				
			I	*B*	*S*	*P*	*L*
Qtz	I	euhedral to subhedral; with undulose extinction	x	x	x*	x	x
	II	euhedral to subhedral; not deformed	x	x	x*	x	x
	III	vermicular; myrmekite intergrowth in Ab	x		x*	x	
Kfs	I	euhedral to subhedral; < 1.3 cm; clear and without weathering	x	x	x*	x	x
	II	subhedral; weathered; with Pl, Ap and Ms inclusions; chess board twining	x	x	x*	x	x
	III	subhedral; perthitic texture		x	x*	x	
	IV	euhedral to subhedral; fractures filled by late Ap and Urn				x	
Ms	I	subhedral flakes; < 1.5 cm; kink bands and bent crystals	x	x	x*	x	
	II	scaly and acicular aggregates; replaces Kfs, Ab, Grt, Spd, Pet and And	x	x	x*	x	x
	III	fish scale shape; Replacing fractures and associated with organic material					
Ab	I	euhedral to subhedral; not deformed	x	x	x	x	x
	II	euhedral to subhedral; deformed presenting bent twining	x	x	x*	x	x
	III	euhedral to subhedral; with myrmekites	x		x*	x	
	IV	anhedral; shredded texture			x*		x
Spd	I	euhedral to subhedral; poikilitic crystals of Spd with sparse blebs of Qtz			x*	x	
	II	fine-grained needles; symplectitic Qtz-Spd surrounds coarser-grained Spd			x*		
	III	fine-grained needles; surrounds Pet, and Ab; overlaps coarser Spd and Qtz				x	
	IV	subhedral to anhedral; SQUI: isochemical breakdown of Pet to Spd+2Qtz			x	x	
Pet	I	euhedral to subhedral; primary; subgranulation; granoblastic texture			x	x	
	II	subhedral; secondary surrounding Spd			x*	x	
Euc	I	anhedral; in the fractures of primary Spd and Pet			x	x	
	II	anhedral; in the fractures of secondary Pet that surrounds Spd			x*	x	
Lpd	I	fine- to coarse-grained mass of interlocking scales; zonal growth with Ms					x
F-Ap	I	subhedral to euhedral; widely distributed	x	x	x*	x	x
	II	subhedral to euhedral hexagonal prisms; as inclusions in Kfs and Cst				x	
	III	anhedral; fills fractures in Kfs				x	
Mnz-(Ce)	I	subhedral; usually associated with Ap-(F)		x		x	
Xnt	I	anhedral; replacing zircon on petalite pegmatites				x	
Atn	I	flakes of euhedral autunite were only identified after heavy liquid separation				x	
Cst	I	subhedral to euhedral; fractured; homogeneous with rare CT inclusions				x	x
	II	subhedral to euhedral; CT, Ap, Zrn, Qtz, Mst, Kfs, Ab, Cook inclusions				x	
Tur	I	subhedral to euhedral; crude layering; especially close to the contacts	x	x			
	II	subhedral; < 1.3 mm; rare occurrence			x*		
Zrn	I	subhedral to euhedral; in Bt with pleochroic halos	x	x			
	II	slender rounded grains; with exsolutions of uraninite	x	x	x	x	x
CT	I	subhedral to euhedral; grains distributed in the pegmatite and aplitic part			x	x	x
	II	subhedral to euhedral; associated with Cst; internal zoning				x	
	III	anhedral; < 7 μm; small globular inclusions in Cst				x	
Py	I	euhedral isolated cubes; < 2 mm		x	x	x	
	II	subhedral; associated with Sp and Py			x		
Sp	I	with Gn inclusions; occurs in interstices or filling of vugs in the aplitic unit			x*		
	II	anhedral; irregular masses and is associated with Py				x	
Urn	I	anhedral to subhedral; associated with Nb-Ta-Sn oxides			x	x	
	II	anhedral; as inclusions in Pet and Kfs				x	
	III	droplets; as exsolutions in Zrn				x	

*- previously described by CHAROY et al. (2001), and LIMA (2000).

Min- mineral; Var- Petrographic variety; Qtz- quartz, Kfs- K-feldspar, Ms- muscovite, Ab- albite, Spd- spodumene, Pet- petalite, Euc- eucryptite, Lpd- lepidolite, F-Ap- fluorapatite, Mnz-(Ce)- monazite-(Ce), Xnt- Xenotime, Atn- autunite, Cst- cassiterite, Tur- tourmaline, Zrn- zircon, CT- columbite-tantalite, Py- pyrite, Sp- spharelite, Gn- galena, Urn- uraninite, Chl- chlorite, Grt- garnet, Bt- biotite, cook- Cookeite.

I – Intragranite pegmatite; B- Barren pegmatite; S- Spodumene pegmatite; P- Petalite pegmatite; L- Lepidolite pegmatite.

Table 3. Representative chemical composition of K-feldspar from the different types of pegmatites.

Pegmatite type	Intra granite	Intra granite	Barren	Barren	Spodu mene	Spodu mene	Petalite	Petalite
Al_2O_3 wt.%	18.41	18.44	18.81	18.79	18.51	18.50	18.58	18.70
SiO_2	64.52	64.49	64.66	64.62	64.54	64.41	64.40	64.40
TiO_2	0.03	0.02	0.01	0.02	0.05	0.04	0.01	0.00
FeO	0.01	0.01	0.00	0.00	0.01	0.01	0.00	0.00
CaO	0.02	0.02	0.00	0.01	0.01	0.00	0.00	0.00
K_2O	15.28	15.44	15.48	15.45	15.50	15.51	15.56	15.49
MgO	0.00	0.00	0.00	0.01	0.01	0.04	0.00	0.00
MnO	0.00	0.00	0.00	0.00	0.01	0.00	0.00	0.00
Na_2O	0.32	0.34	0.28	0.32	0.32	0.22	1.05	0.67
P_2O_5	0.01	0.02	0.02	0.02	0.01	0.02	0.00	0.00
BaO	0.02	0.02	0.01	0.02	0.01	0.01	0.00	0.00
ZnO	0.00	0.00	0.00	0.00	0.00	0.00	0.00	0.00
Rb_2O	0.36	0.38	0.31	0.33	0.28	0.29	0.39	0.41
Cs_2O	0.04	0.03	0.03	0.03	0.02	0.02	0.02	0.02
Total	99.02	99.22	99.62	99.61	99.28	99.08	100.00	99.68
Apfu on the basis of 8 atoms of oxygen								
Al apfu	1.021	1.022	1.037	1.036	1.025	1.026	1.025	1.033
Si	2.992	2.988	2.981	2.980	2.987	2.986	2.972	2.975
Ti	0.001	0.001	0.000	0.001	0.002	0.001	0.000	0.000
Fe^{2+}	0.000	0.000	0.000	0.000	0.000	0.000	0.000	0.000
Ca	0.001	0.001	0.000	0.000	0.000	0.000	0.000	0.000
K	0.918	0.927	0.924	0.922	0.929	0.931	0.929	0.926
Mg	0.000	0.000	0.000	0.001	0.000	0.003	0.000	0.000
Mn	0.000	0.000	0.000	0.000	0.000	0.000	0.000	0.000
Na	0.029	0.031	0.026	0.029	0.029	0.020	0.095	0.060
P	0.001	0.001	0.001	0.001	0.000	0.001	0.000	0.000
Ba	0.000	0.000	0.000	0.000	0.000	0.000	0.000	0.000
Zn	0.000	0.000	0.000	0.000	0.000	0.000	0.000	0.000
Rb	0.011	0.011	0.009	0.010	0.008	0.009	0.012	0.012
Cs	0.001	0.001	0.001	0.001	0.000	0.000	0.000	0.000
Z	4.01	4.01	4.02	4.02	4.01	4.01	4.00	4.01
X	0.96	0.97	0.96	0.96	0.97	0.97	1.04	1.00
K/Rb	38.52	36.87	45.31	42.49	50.23	48.53	36.21	34.29
%An	0.10	0.11	0.00	0.05	0.05	0.00	0.00	0.00
%Ab	3.10	3.26	2.71	3.00	3.06	2.10	9.26	6.13
%Or	96.80	96.63	97.29	96.95	96.89	97.90	90.74	93.87

apfu- atoms per formula unit; An- anorthite; Ab- albite; Or- orthoclase.

Table 4: Representatitve chemical composition for the albite from the studied pegmatites.

Pegmatite type	Intra granite	Barren	Petalite	Lepidolite
MgO (wt.%)	0.00	0.00	0.00	0.00
Al_2O_3	19.62	19.70	19.59	19.64
SiO_2	68.55	68.65	68.64	68.73
TiO_2	0.00	0.00	0.01	0.00
FeO	0.00	0.00	0.00	0.00
CaO	0.14	0.14	0.08	0.06
K_2O	0.04	0.03	0.04	0.03
MnO	0.00	0.00	0.00	0.00
Na_2O	11.40	11.40	11.55	11.53
P_2O_5	0.00	0.00	0.00	0.00
BaO	0.00	0.00	0.00	0.00
ZnO	0.00	0.00	0.00	0.00
Total	99.75	99.79	99.92	99.99
Apfu on the basis of 8 atoms of oxygen				
Mg (apfu)	0.000	0.000	0.000	0.000
Al	1.022	1.024	1.019	1.021
Si	2.985	2.984	2.986	2.986
Ti	0.000	0.000	0.000	0.000
Fe^{2+}	0.000	0.000	0.000	0.000
Ca	0.007	0.006	0.004	0.003
K	0.002	0.002	0.002	0.002
Mn	0.000	0.000	0.000	0.000
Na	0.977	0.975	0.988	0.986
P	0.000	0.000	0.000	0.000
Ba	0.000	0.000	0.000	0.000
Zn	0.000	0.000	0.000	0.000
%An	0.68	0.63	0.39	0.28
%Ab	99.07	99.09	99.39	99.56
%Or	0.33	0.28	0.23	0.16

apfu- atoms per formula unit; An- anorthite; Ab- albite; Or- orthoclase

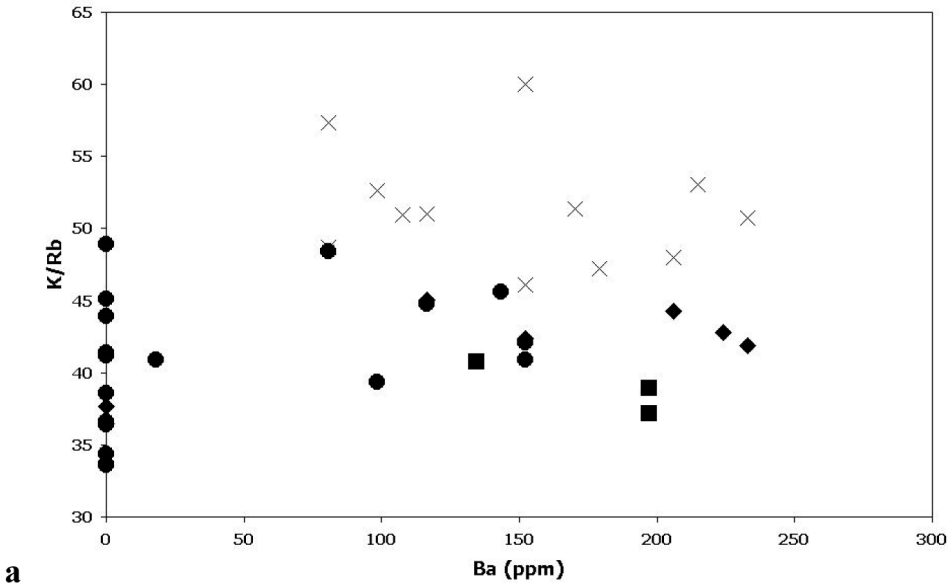

a

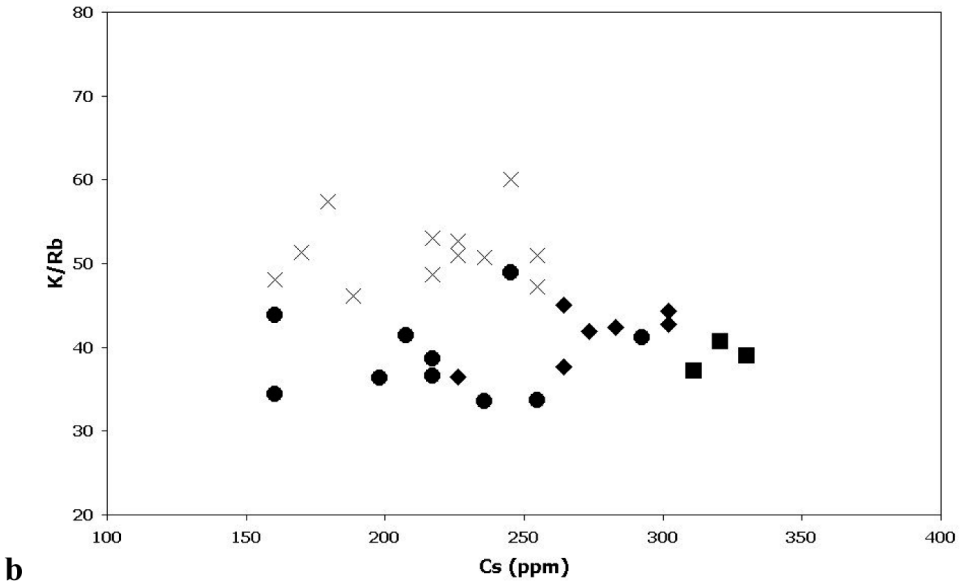

b

Fig. 5. Charts representing the variation of K/Rb ratio with Ba, Cs, and Rb for the different types of pegmatites (a-c). Plotted with data from EPMA. All values in ppm. Pegmatite types as described previously. (continued...)

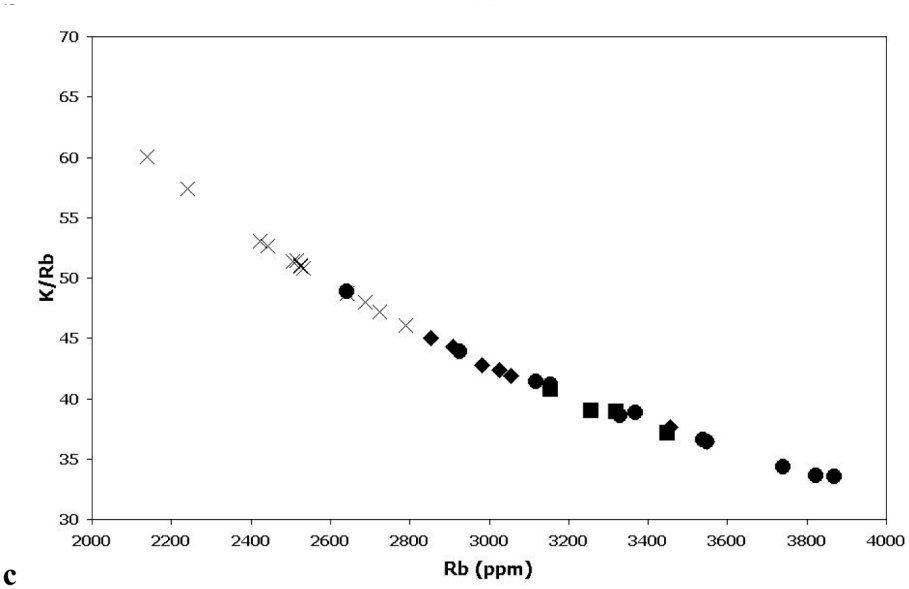

c

As it is possible to observe in Table 3 and Figure 5, our predictions were not observed. Unfortunately it is not possible to see geochemistry evolution taking into consideration the concentration of incompatible elements or the decrease in the K/Rb ratio (Figure 5 and Table 3). This may be due to K-feldspar incapacity of keeping its primary chemical attributes or they were modified or lost as argued by LONDON (2008).

Micas

Muscovite is found in all the pegmatites types described for Barroso-Alvão, whereas other type of micas such as biotite, chlorite, and lepidolite are exclusive of certain groups of pegmatites. Biotite and chlorite were only observed in intragranite, and barren pegmatites; lepidolite is only observed in lepidolite pegmatites. Detailed petrographic characterization can be found in Table 2.

Table 5 presents representative chemical composition of the studied micas for the different types of pegmatites. It was selected primary muscovite from all of the different types of pegmatites. The different studied muscovite has chemical compositional variation, as it is possible to observe in Figure 6 and Table 5. BSE imaging of the studied muscovite does not show chemical zoning and quantitative analyses show constant chemical composition either on their cores and rimes.

It is possible to observe that the muscovites from intragranite, barren, and petalite pegmatites present a variation in their Al content. Micas from lepidolite pegmatites are the most impoverished in FeO and MgO. Trace element content shows differences between the micas from the different types of pegmatites (Figure 6). Lepidolite is the richest in Rb (4682 – 5596 ppm), Cs (424 – 565 ppm), F (44460 – 55520 ppm),

and Li (12246 – 21842 ppm). Intragranite pegmatites are the most enriched in TiO2 (0.02 – 0.03 wt.%), FeO (1.32 – 1.46 wt.%), and MnO (0.03 – 0.05 wt.%), and the most depleted in Rb (2094 – 3145 ppm), Cs (170 – 311 ppm) (MARTINS, 2009).

Table 5: Representative chemical composition of the EMPA analyses in muscovite from the studied pegmatites.

	Intra granite	Barren	Spodumene	Petalite	Lepidolite
SiO_2 (wt.%)	47.36	46.85	45.86	46.83	50.22
TiO_2	0.02	0.02	0.01	0.01	0.00
Al_2O_3	34.90	35.97	37.89	36.63	27.11
FeO	1.42	0.93	1.08	1.19	0.01
MnO	0.04	0.03	0.02	0.04	0.21
MgO	0.02	0.03	0.02	0.02	0.00
CaO	0.03	0.03	0.03	0.03	0.10
Li_2O *	0.78	0.38	0.05	0.27	3.61
Na_2O	0.11	0.11	0.09	0.09	0.30
K_2O	9.45	9.42	9.88	9.92	9.60
Rb_2O	0.32	0.35	0.44	0.44	0.57
Cs_2O	0.03	0.03	0.03	0.03	0.05
F	1.73	1.62	1.47	1.59	2.48
Total 1	96.21	95.76	96.63	97.10	94.26
O=F	0.73	0.68	0.62	0.67	1.05
Total 2	95.48	95.08	96.01	96.43	93.22
Apfu in the basis of 22 oxygens					
Si (apfu)	6.191	6.052	5.901	6.001	6.485
$Al^{(IV)}$	1.809	1.948	2.099	1.999	1.515
Sum Z	8.00	8.00	8.00	8.00	8.00
Ti	0.002	0.002	0.001	0.001	0.000
$Al^{(VI)}$	3.568	3.529	3.647	3.533	2.611
Fe^{2+}	0.156	0.101	0.116	0.127	0.001
Mn	0.004	0.003	0.003	0.005	0.023
Mg	0.005	0.005	0.004	0.005	0.000
Li	0.412	0.201	0.027	0.168	1.917
Sum Y	4.15	4.17	3.96	4.01	4.80
Ca	0.004	0.004	0.003	0.004	0.014
Na	0.028	0.027	0.024	0.023	0.074
K	1.576	1.552	1.621	1.622	1.581
Rb	0.027	0.029	0.036	0.037	0.048
Cs	0.002	0.001	0.002	0.002	0.003
Sum X	1.64	1.61	1.69	1.69	1.72
F	0.714	0.661	0.596	0.645	1.014
K (ppm)	78403	78170	81954	82304	79620
Rb	2926	3160	3992	4056	5234
K/Rb	27	25	21	20	15
Cs	255	252	315	262	509
Li	3640	1768	238	1275	16758

apfu- atoms per formula unit; *- calculated using the equation
$Li_2O = (3.735*F) – 5.6669$ ($R^2= 0.9705$; n= 6) according to TISCHENDORF et al. (1999)

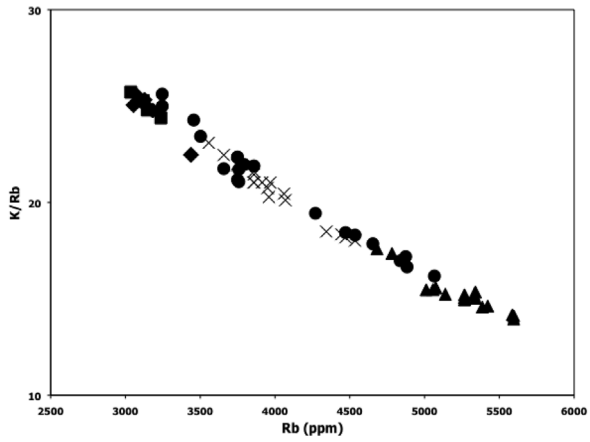

Fig. 6. Variation of the K/Rb ratio with Rb for micas from the different types of pegmatites. Pegmatite types: square- Intragranite pegmatites; diamond- Barren pegmatites; cross- Spodumene pegmaites; circle- Petalite pegmatites; triangle- Lepidolite pegmatites.

The K/Rb ratio, and the enrichment in incompatible elements such as Li, Cs, and Cs, are one of the most valuable indicators of fractionation in micas (ČERNÝ et al. 1985). With fractionation, the K/Rb ratio tends to decrease. On the other hand, the enrichment of incompatible elements tends to increase. In this study we observe decreasing of the K/Rb ratio in the studied micas in intragranite pegmatites towards the lepidolite pegmatites (Figure 6). Thus, using this indicator it is possible to observe that the intragranite pegmatites are the most primitive and the lepidolite pegmatites, the most evolved. Spodumene pegmatites, and petalite pegmatites have similar evolution indicators.

Nb-Ta-Sn oxides

In the area it was reported frequent occurrence of cassiterite in the greisens surrounding the pegmatites, exploited for tin on a small scale after the Second World War. CHAROY et al. (1992) describes lepidolite aplite-pegmatite veins exhibiting low-grade tin mineralization (0.1 to 0.3 vol. %). Those veins were mined, wherever argilitic alteration made digging by hand possible. This type of cassiterite was not found thus it is not characterized in this study. The studied cassiterite is observed in petalite pegmatites and lepidolite pegmatites. It is considered primary based on petrographic and microtextural observation.

In petalite pegmatites, cassiterite is chemically homogenous (SnO_2 content varying from 94.24 to 99.01 SnO_2 wt.%) even when close to the smallest identified inclusion of columbite group minerals (CGM). Table 6 shows representative analyses of cassiterite from petalite pegmatites and lepidolite pegmatites. It is possible to observe that cassiterite from petalite pegmatites is enriched in Nb_2O_5, Ta_2O_5, MnO, FeO, and WO_3 when compared with the cassiterite from lepidolite pegmatites that is almost 100 wt.% SnO_2.

Table 6. Representative chemical composition of electron microprobe (EPMA) analyses of cassiterite from petalite pegmatites and lepidolite pegmatites.

Pegmatite type	Petalite	Lepidolite
WO_3 (wt.%)	0.15	0.00
Ta_2O_5	1.34	0.18
Nb_2O_5	0.27	0.04
TiO_2	0.17	0.03
SnO_2	97.61	98.74
FeO	0.33	0.21
MnO	0.16	0.04
MgO	0.03	0.05
CaO	0.00	0.00
Total	100.05	99.28
Atoms per formula unit calculated based on 4 oxygens		
W (apfu)	0.002	0.000
Ta	0.018	0.002
Nb	0.006	0.001
Ti	0.007	0.001
Sn	1.948	1.987
Fe	0.014	0.009
Mn	0.007	0.002
Mg	0.002	0.003
Ca	0.000	0.000

n- number of analyses; apfu- atoms per formula unit

Columbite group minerals (CGM) are only present in the Li-enriched pegmatites: spodumene, petalite, and lepidolite (Figure 7). CGM are considered of primary crystallisation based on petrography and microtextures observation. CGM show complex internal chemical composition with Nb- and Ta-rich cores and rimes. This suggests crystallisation at disequilibrium. In spodumene and lepidolite pegmatites CGM minerals only appear as discrete grains in the aplitic and pegmatitc ground mass. In the petalite pegmatites the CGM grains are found in the ground mass as well, and as inclusions in cassiterite. These minerals are inclusions and not exsolutions because it is not observed a decreasing in the Nb_2O_5 and Ta_2O_5 content of the host cassiterite when close to the CGM grains.

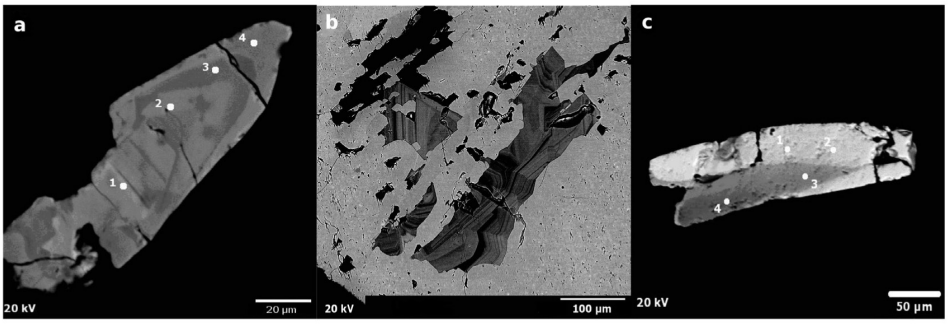

Fig. 7. BSE imaging of different aspects of CGM from the Li-enriched pegmatites. CGM has complex chemical zoning. In the CGM inclusions, the darkest areas correspond to Nb enrichment, and the brightest areas correspond to the Ta enrichment. (a) Elongated CGM with an oscillatory growth pattern. Numbers 1 to 4 represent the analysed areas of the crystal. In this example we have a Ta rich core, surrounded by Nb rich concentric zones, and a Ta enriched rime. (b) Skeletal CGM evidencing sharp contacts with the host cassiterite (light grey colour). (c) CGM from a lepidolite pegmatite.

All of the CGM of the three types of pegmatites exhibit variable and distinct chemical composition expressed in Table 7, and can be classified as columbite-(Fe), tantalite-(Fe), and columbite-(Mn). The SnO_2 content in all the discrete CGM from all the different types of pegmatites is constant and very close to 0%wt. Except for the CGM minerals described as inclusions in cassiterite from the petalite pegmatites; these are the most enriched in SnO_2. The CGM minerals from spodumene pegmatites are the most enriched in TiO_2 that gradually decreases towards the lepidolite type (Table 7).

Table. 7. Representative analyses of discrete grains of columbite-(Fe) from spodumene pegmatites; columbite–(Fe) grain included in cassiterite (Cst) and discrete columbite grains from petalite pegmatites; discrete grains of strongly Mn–enriched columbite–(Mn) and tantalite–(Mn) from lepidolite pegmatites.

Pegmatite type	**Spodumene**		**Petalite**		**Lepidolite**	
	discrete grains		**incl. in Cst**	**discrete grains**	**discrete grains**	
MnO wt.%	4,57	4,98	4,78	4,43	15,81	17,59
FeO	13,38	13,89	12,54	12,44	0,17	0,18
Ta_2O_5	43,80	32,21	49,65	38,54	60,93	41,62
Nb_2O_5	34,56	43,96	31,90	42,68	23,75	40,45
SnO_2	0,03	0,03	0,02	0,00	0,01	0,01
TiO_2	3,22	3,12	0,79	1,68	0,00	0,00
WO_3	0,31	0,29	0,16	0,19	0,25	0,20
Total	99,87	98,49	99,90	100,01	100,92	100,07
A site						
Mn	1,046	1,098	1,134	0,988	3,928	4,012
Fe^{2+}	3,025	3,026	2,940	2,738	0,041	0,041
B site						
Ta	3,221	2,281	3,784	2,758	4,861	3,049
Nb	4,224	5,175	4,041	5,077	3,150	4,925
Sn	0,003	0,003	0,002	0,000	0,001	0,001
Ti	0,656	0,612	0,166	0,332	0,000	0,000
W	0,022	0,019	0,012	0,013	0,019	0,014
Mn/(Mn+Fe)	0,26	0,27	0,28	0,27	0,99	0,99
Ta/(Ta+Nb)	0,43	0,31	0,48	0,35	0,37	0,38

Cation formula based on 24 atoms of oxygen. Oxides in wt.%

In what respect to fractionation, there is an overlapping of the CGM for the spodumene pegmatites and the ones hosted in cassiterite from the petalite pegmatites (Figure 8). The Mn and Ta content increases from the CGM minerals of the spodumene pegmatites and the inclusions from the petalite pegmatites towards the lepidolite pegmatites. From Figure 8, it is possible to observe that the trend starts from the region Mn-poor columbite-(Fe) towards a slightly Mn- and Ta- enriched columbite-(Fe) and tantalite-(Fe). The Ta/(Ta+Nb) values are maintained and enters the field of columbite-(Mn) and tantalite-(Mn) as the Mn/(Mn+Fe) ratio approaches 1.0 for the lepidolite pegmatites.

CGM from Barroso-Alvão can be used to observe regional geochemical fractiona-

tion taking into account the Li-enriched pegmatites. We propose a higher degree of fractionation for the lepidolite pegmatites based on the Mn/(Mn+Fe) and Ta/(Ta+Nb) ratios observed in this pegmatite's CGM.

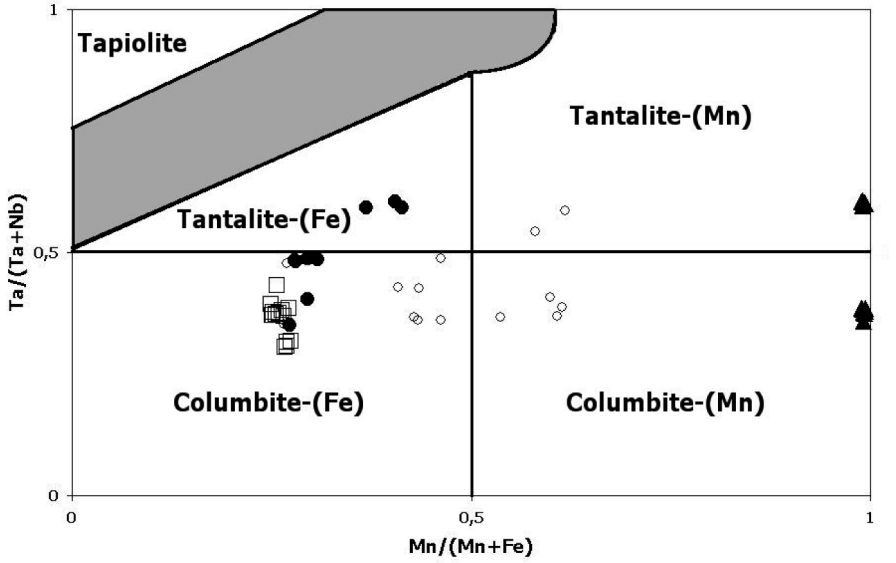

Fig. 8. Compositions of CGM from the three different pegmatite types plotted in the quadrilateral diagram columbite-(Fe), columbite-(Mn), tapiolite, tantalite-(Mn). The dashed arrow indicates the evolution compositional trend. Open squares: discrete CGM from spodumene pegmatites; Open circles: CGM inclusions in cassiterite from petalite pegmatites; Filled circles: discrete CGM from petalite pegmatites; Triangles: discrete CGM from lepidolite pegmatites.

CONCLUDING REMARKS

The pegmatite bodies of the Barroso-Alvão pegmatite field were studied taking into account several parameters, which allowed a division into different groups. The pegmatite field has a rare-element enrichment with major enrichment in Li, Rb, Be, Sn, Nb, and Ta. Enrichment in Ga, B and Cs is not observed.

Regional zoning in this pegmatite field is not easy to observe but it seems to be related with the syn-D_3 granitic intrusions in the area. One cannot forget the two dimensional limitations of schematically representations in a plan view compared to a three-dimensional approach. For example, just by having a different position of the erosion level it is possible to observe different fractionated patterns outcropping. Another example to observe this, and considering the same erosion level, will be the existence of a basement of granitic massifs structures in domes not observed outcropping (RODA-ROBLES et al., 2007).

Muscovite was the mineral where the degree of fractionation was evaluated more efficiently amongst all the studied pegmatite types. In muscovite, the K/Rb ratio decreases with fractionation. From the mica study,

it is possible to observe that the evolution increases from intragranite pegmatites towards the lepidolite pegmatites. Muscovites from intragranite pegmatites are the most primitive with the highest K/Rb ratio. The lepidolite from the lepidolite pegmatites has the lowest K/Rb value of the studied pegmatites, thus they are considered the most evolved.

Columbite group minerals can be used to observe regional geochemical fractionation for the Li-enriched pegmatite bodies of the Barroso-Alvão pegmatite field. CGM from the spodumene pegmatites and CGM inclusions in cassiterite from the petalite pegmatites have a similar chemical composition. However, the CGM discrete grains from the petalite pegmatites are more MnO enriched. Even if there it is observed a similar Ta_2O_5 content for the CGM in pegmatites, it is proposed a higher degree of fractionation for petalite pegmatites based on the MnO enrichment. Mn/(Mn+Fe) and Ta/(Ta+Nb) ratios are higher for lepidolite pegmatites than for the spodumene pegmatites and petalite pegmatites. These observations allow proposing a higher degree of evolution for the lepidolite pegmatite.

Based on mineral geochemistry it is possible to observe a trend between intragranite pegmatites, barren pegmatites, spodumene pegmatites, petalite pegmatites, and lepidolite pegmatites. We consider the intragranite and barren pegmatites less evolved whereas the Li-bearing ones are highly evolved, and rare-element rich. Nonetheless the fractionation process is not completely understood in Barroso-Alvão. It is undeniable there is evolution in this pegmatite field but there are not enough data to sustain that the observed evolution is only related with a single fractionation process as already stated by CHAROY & NORONHA (1999). This is in part due to the severe weathering that affects the studied lepidolite pegmatite. Further studies are required to get a better understanding of the fractionation process in Barroso-Alvão and trying to define the relationship between the pegmatites and the larger granite bodies that outcrop in the region.

ACKNOWLEDGMENTS

This work is part of a PhD thesis and benefited from financial support from Fundação para a Ciência e Tecnologia, Portugal. The first author would like to acknowledge all opportunities created by her adviser, and all of the shared knowledge and time spent abroad with scientists from different Universities. The authors would like to express appreciation to William Simmons, Karen Webber and Al Falster at University of New Orleans, USA for the analyses and numerous discussions. Comments from Fernando Noronha are truly acknowledged

REFERENCES

ALFONSO P., MELGAREJO J., YUSTA I. and VELASCO I. (2003). Geochemistry of feldspars and muscovite in granitic pegmatite from the Cap de Creus Field, Catalonia, Spain. *Canadian Mineralogy* 41, 103-116.

ALMEIDA A. (1994). *Geoquímica, petrogénese e potencialidades metalogénicas dos granitos peraluminosos de duas micas do complexo de Cabeceiras de Basto. (Geochemistry, petrogenises and metalogenetic potencial of the two mica peraluminous Cabeceiras de Basto granitic complex).* Ph. D. thesis. University of Porto, Portugal. 305 p. (in Portuguese).

ALMEIDA A., MARTINS H. C. and NORONHA F. (2002). Hercynian Acid Magmatism and Related Mineralizations in Northern Portugal. *Gondwana Research* 5 (2), 423-434.

AMARANTE M. M., BOTELHO DE SOUSA A. and MACHADO LEITE M. (1999). Technical note: Processing a spodumene ore to obtain lithium concentrates for addition to glass and ceramics bodies. *Minerals Engineering* 12 (4), 433-436.

Carta Geológica de Portugal, escala 1:50.000, Folha 6A - Montalegre. *Instituto Geológico e Mineiro*, Lisboa, 1987. (in Portuguese).

Carta Geológica de Portugal, escala 1:50.000, Folha 6B – Chaves, *Serviços Geológicos de Portugal, Lisboa*, 1967. (in Portuguese).

Carta Geológica de Portugal, escala 1:50.000, Folha 6C – Cabeceiras de Basto, *Serviços Geológicos de Portugal/Instituto Geológico e Mineiro*, Lisboa, 1998. (in Portuguese).

Carta Geológica de Portugal, escala 1:50.000, Folha 6D – Vila Pouca de Aguiar, Serviços *Geológicos de Portugal/ Instituto Geológico e Mineiro*, Lisboa, 1998. (in Portuguese).

ČERNÝ P. and FERGUSON R. B. (1972). The Tanco Pegmatite at Bernic Lake, Manitoba. IV Petalite and Spodumene relations. *Can. Mineral.* **11**, 660-678.

ČERNÝ P., MEINTZER R. and ANDERSON A. (1985) Extreme fractionation in rare element granitic pegmatites: selected examples of data and mechanisms. *Can. Mineral.* **23**, 381-421.

CHAROY B., LOTHE F., DUSAUSOY Y. and NORONHA F. (1992). The Crystal Chemistry of Spodumene in some Granitic Aplite-Pegmatite from Northern Portugal. *Canadian Mineralogy.* 30, 639-651.

CHAROY, B. and NORONHA, F. (1999). Rare-element (Li-rich) granitic bodies: A primary or a superimposed signature?. *Revista Brasileira Geociências*, 29, (1) 3-4, 1-8.

CHAROY, B. and NORONHA, F. (1988). A espodumena como fase litinifera de aplitopegmatitos da região de Covas de Barroso (Norte de Portugal). In: *X Reunião sobre a Geologia do Oeste Peninsular. (Salamanca e Coimbra 1988)* Resumos das Comunicações.

CHAROY, B., NORONHA, F. and LIMA, A.M.C. (2001). Spodumene-Petalite-Eucryptite: mutual relationships and alteration style in pegmatite-aplite dykes from Northern Portugal. *Canadian Mineralogy* 39, 729-746.

DIAS, R. and RIBEIRO, A. (1995). The Ibero-Armorican Arc: A collision effect against an irregular continent? *Tectonophysics* 246, 113-128.

DONOVAN, J. J. and TINGLE, T. N. (1996). An Improved Mean Atomic Number Background Correction for Quantitative Microanalysis. *Microscopy and Microanalysis* 2 (1), 1-7.

DÓRIA A., CHAROY B. and NORONHA F. (1989). Fluid inclusion studies in spodumene-bearing pegmatite-aplite dykes of Covas de Barroso, Northern Portugal. ECROFI X (London) *Program Abstr.*, 25.

FARIAS, P., GALLASTEGUI, G., GONZÁLEZ LODEIRO, F.; MARQUÍNEZ, J., MARTÍN PARRA, L. M., MARTÍNEZ CATALÁN, J. R., DE PABLO MACIÁ, G. and RODRÍGUEZ FERNÁNDEZ, L. (1987). Aportes al conocimiento de la litoestratigrafía y

estructura de Galicia Central. (Insights on the lithostratigraphy and struture of the Central Galicia) IX Reunião de Geologia do Oeste Peninsular. *Publicação do Museu e Laboratório Mineralógico e Geológico da Faculdade de Ciências, Universidade do Porto,* Program Abstr. 1, 411-431. (in Spanish).

FARINHA, J. and LIMA, A. (2000). Estudo dos Filões Aplitopegmatíticos Litiníferos da Região do Barroso Alvão (Norte de Portugal) (Study of the Lithium rich aplite pegmatite bodies from the Barroso-Alvão region-Northern Portugal). *Estudos, Notas e Trabalhos* 42, 48 p. (in Portuguese).

FERREIRA, N., IGLESIAS, M., NORONHA, F., PEREIRA, E., RIBEIRO, A. and RIBEIRO, M. L. (1987). Granitoides da Zona Centro Ibérica e o seu enquadramento geodinâmico. (Granitoids from the Central Iberian Zone and their geodynamical setting) *In*: *Geologia de los Granitoides y Rocas Asociadas del Macizo* (Bea F. et al., eds.). Libro Homenaje a L.C. Garcia de Figuerola 37-51. (in Portuguese).

LARSEN, R. B. (2002). The distribution of rare-earth elements in K-feldspar as an indicator of petrogenetic proceses in granitic pegmatites: examples from two pegmatite fields in Sourthern Norway. *Canadian Mineraology.* 40, 137-151

LIMA, A. (2000). *Estrutura, Mineralogia e Génese dos Filões Aplitopegmatíticos com Espodumena da Região do Barroso-Alvão (Norte de Portugal)*. (Structure, Mineralogy and genesis of the spodumene-rich aplite pegmatite bodies from Barroso-Alvão-Northern Portugal) *Ph. D. thesis. University of Porto, Portugal and INPL, Nancy, France*, 270 p. (in Portuguese).

LIMA, A., VIEIRA, R., MARTINS, T., NORONHA F. and CHAROY B. (2003a). A ocorrência de petalite como fase litinífera dominante em numerosos filões do campo aplitopegmatítico do Barroso-Alvão (N. de Portugal). (Petalite occurrence as a dominant lithium phase in numerous pegmatite bodies from the Barroso-Alvão pegmatite field-Northern Portugal). *CD-Rom of the VI CNG, Almada, Portugal, Program Abstr.* **V**. (in Portuguese).

LIMA, A. M. C., VIEIRA, R. C., MARTINS, T. C., FARINHA, J. A., NORONHA, F. M. P. and CHAROY, B. (2003b). Os filões aplitopegmatíticos litiníferos da região Barroso-Alvão (Norte de Potugal). (Lithium-rich aplite pegmatite bodies from Barroso-Alvão region) Publicação do Departamento de Ciências da Terra e do Museu Mineralogia e Geologia, Universidade de Coimbra. *Memórias e Notícias* 2 (Nova Série),173-194. (in Portuguese).

LIMA, A. M. C., VIEIRA, R., MARTINS, T. and NORONHA, F. (2003c). Aplicação de geoquímica de sedimentos de linhas de água na prospecção de filões aplitopegmatíticos litiníferos no campo aplitopegmatítico do Barroso-Alvão (Norte de Portugal). (Using stream sediment geochemistry for exploration of aplite-pegmatite bodies from Barroso-Alvão-Northern Portugal) *Actas do IV Congresso Ibérico de Geoquímica, Universidade de Coimbra*, 468-460. (in Portuguese).

LONDON, D. (2008). Pegmatites. *Canadian Mineralogy, Special Publication* 10, 347 p.

MARTINS, H. C.B, SANT'OVAIA, H. and NORONHA, F., (2009). Genesis and emplacement of felsic Variscan plutons within a deep crustal lineation, the Penacova-

Regua-Verin fault: An integrated geophysics and geochemical study (NW Iberian Peninsula) *Lithos*, 111 (3-4): 142-155

MARTINS, T. (2009). *Multidisciplinary study of pegmatites and associated Li and Sn-Ta-Ta mineralisation from the Barroso-Alvão region*. PhD thesis, Porto University, Portugal.

MARTINEZ, F. J., CORRETGE, L. G. and SUAREZ, O. (1990). Distribution, Characteristics and Evolution of Metamorphism. *In*: *Pre-Mesozoic Geology of Iberia* (R.D. Dallmeyer & E. Martínez Garcia eds.) 207-211.

NEIVA, A. M. R. (1995). Distribution of trace elements in feldspars of granitic aplites and pegmatites from Alijo–Sanfins, northern Portugal. *Mineralogical Magazine* 59, 35-45.

NORONHA, F. (1983). *Estudo Metalogénico da área Tungstífera da Borralha*. Ph. D. thesis. University of Porto, 413p. (in Portuguese).

NORONHA, F. (1987). Nota sobre a ocorrência de filões com espodumena na folha de Dornelas. (Occurrence of pegmatite bodies with spodumene in the Dornelas geological map). *Portuguese Geological Survey Internal report.* (in Portuguese).

NORONHA, F. and CHAROY, B. (1991). Pegmatitos graníticos com elementos raros da região de Barroso (Norte de Portugal) (Granitic pegmatites with rare element mineralisation from the Barroso region (North Portugal). *Resumos do Congresso de Geoquímica dos Países de Língua Portuguesa. University of S. Paulo* **1**, 276-279. (in Portuguese).

NORONHA, F., RAMOS, J. M. F., REBELO, J., RIBEIRO, A. and RIBEIRO, M. L. (1981). Essai de corrélation des phases de déformation hercyniennes dans le NW de la P.I.. *Leidse Geologische Mededelingen* 52 (1), 87-91.

NORONHA, F. and RIBEIRO, M. L. (1983). Notícia Explicativa da Folha 6-A, Montalegre. *Serviços Geológicos de Portugal, Lisboa*, 29 p.

PIRES, M. (1995). Prospecção Geológica e Geoquímica. Relatório interno da Prospecção de Jazidas Litiníferas e de Metais Associados entre as Serras de Barroso e Alvão - Ribeira de Pena. (Geological and Geochemical exploration of Li deposits in Barroso-Alvão - Ribeira de Pena. Internal report of the Portuguese Geological Survey) IGM, Lisboa, 46 p (in Portuguese).

RIBEIRO, M. A. (1998) Estudo litogeoquímico das formações metassedimentares encaixantes de mineralizações em Trás-os-Montes Ocidental. Implicações metalogénicas. (Lithogeochemical study of the metasedimentary country rock that hosts mineralisation in Trás-os-Montes Ocidental. Metalogenetic implication.) Ph D. thesis. University of Porto, Portugal, 231p.

RIBEIRO, M. A., MARTINS, H. C., ALMEIDA, A. and NORONHA, F. (2000). Carta Geológica de Portugal, escala 1:50 000, 6-C (Cabeceiras de Basto), *Notícia Explicativa, Serviços Geológicos de Portugal,* 48 p. (in Portuguese).

RIBEIRO, M. A., RAMOS, R. and NORONHA, F. (2007). Pegmatite-aplite veins of Barroso-Alvão field. Lithostratigraphy and metamorphism of host rocks. In: Granitic Pegmatites: the state of the art (A. Lima & E. Roda-Robles eds.), Fieldtrip guidebook, Memórias 9, 39-45. Available online http://www.fc.up.pt/peg2007/.

RODA-ROBLES, E. (1993). *Distribucion, caracteristicas y petrogenesis de las pegmatitas de La Fregeneda (Salamanca)*. (Distribution, characteristics and petrogenesis of the pegmatite bodies from La Fregeneda-Salamanca) Ph. D. thesis. University of the Basque Country, Spain. 199 p. (in Spanish).

RODA, E., KELLER, P., PESQUERA, A. and FONTAN, F. (2007). Micas of the muscovite – lepidolite series from Karibib pegmatites, Namibia. *Mineralogical Magazine*, 71, 41 - 62.

TISCHENDORF, G., GOTTESMAN, B. and FÖRSTER, H. J. (1999). The correlation between lithium and magnesium in trioctahedral micas:improved equations for Li_2O estimation from MgO data. Mineral. Mag. 63, 57 - 7.